INVESTIGATION OF NASCAR RESTRICTOR PLATE MANIFOLD INSERT USING WAVE ENGINE SIMULATION AND RESPONSE SURFACE METHODOLOGY

by

JOHN M. GROSS III
B.S. Texas A&M University, 2002

A thesis submitted in partial fulfillment of the requirements
for the degree of Master of Science
in the Department of Industrial Engineering and Management Systems
in the College of Engineering and Computer Science
at the University of Central Florida
Orlando, Florida

Summer Term
2004

ABSTRACT

With the increasing growth in computer processing power, computer based computational fluid dynamics simulations are finding increasing acceptance and use in the field of internal combustion engine development. Once fully developed, such simulations provide detailed and expedient tools for testing existing theories, as well as new ideas.

While numerous studies on wave propagation and fluid flow in intakes manifolds exist, most restrict the analysis to a single intake runner and port, examining only the dynamics from the runner-to-plenum junction downstream to the valve. While such analyses provide comprehensive models for wave propagation dynamics in the runner, little is published on the fluid dynamics and wave propagation in the plenum, and the interactions between runners when an intake manifold's geometric constraints prevent symmetry in the manifold.

This paper will examine the modeling of a 2003 specification Dodge Motorsports NASCAR Restrictor Plate engine using Ricardo's WAVE engine simulation computational fluid dynamics software. This examination will include an introduction to the software and required engine data for constructing a comprehensive model, the process used to validate the simulation's output with acquired engine performance data, and the use of response surface methodology to optimize the dimensions of the plenum insert associated junction. Additionally, an analysis of the problems with modeling this area of the manifold using one-dimensional CFD will be conducted, as well as a discussion of the theories surrounding the insert. Finally, a new hypothesis regarding the insert as well as future work to examine this hypothesis will be introduced.

ACKNOWLEDGMENTS

The authors would like to acknowledge Dodge Motorsports, Evernham Motorsports, and Arrington Racing Engines for their invaluable contributions of time, expertise, and equipment during the course of this research.

TABLE OF CONTENTS

LIST OF FIGURES

LIST OF TABLES

LIST OF ABBREVIATIONS

α - Alpha — scalar of the axial points relative to the cubic points of the design matrix

ACF – constant term in Chenn-Flynn Friction Correlation

BCF – linear coefficient in Chenn-Flynn Friction Correlation, multiplied by Pmax

BHP - Brake Horsepower

BMEP — Brake Mean Effective Pressure

CCD — Central Composite Design

CCF - linear coefficient in Chenn-Flynn Friction Correlation, multiplied by MPS

CFD — Computational Fluid Dynamics

DC — Discharge Coefficient

IVC — Intake Valve Closing point

IVO — Intake Valve Opening point

MEP — Mean Effective Pressure

MPS – mean piston speed

Pmax – peak in-cylinder pressure

QCF – quadratic term in Chenn-Flynn friction correlation, multiplied by MPS^2

RSM — Response Surface Methods

Xl — equivalent diameter of insert window for cylinders 1 and 8

X2 — equivalent diameter of insert window for cylinders 2 and 7

X3 — equivalent diameter of insert window for cylinders 3, 4, 5 and 6

X4 — equivalent diameter of the upstream end of runners 1 and 8

X5 - equivalent diameter of the upstream end of runners 2 and 7

X6 - equivalent diameter of the upstream end of runners 3, 4, 5, and 6

CHAPTER ONE: INTRODUCTION

In any form of auto racing, the ability to quickly and efficiently develop engines for power and reliability is a key determinant in that team's success and ability to continue racing. The inability to find power and reliability results in races lost. The inability to find power and reliability in an efficient manner results in excessive time and cost. Over time, such inefficiencies lead to the demise of a racing team.

In recent years, the dramatic growth in computer processing power has resulted in a corresponding growth in computational fluid dynamics software packages. One such software package, Ricardo's WAVE, is a one-dimensional CFD software suite designed specifically for modeling internal combustion engines. WAVE uses an iterative solver algorithm to solve the boundary conditions and governing equations for the entire engine model, as defined by the modeler. Though three-dimensional CFD software suites exist, as of the writing of this paper, none were capable of dealing with two-phase fluid flow, a critical component of an internal combustion engine.

The traditional method of engine development, particularly in NASCAR racing, is the "cut and fit" method, whereby an idea or theory is tested simply by building a new part and physically testing it in a running engine. While the results of such tests are informative and have led to substantial improvements in power and reliability, the time and cost of such experimentation is quickly becoming prohibitive in today's fast-paced computerized world where computer programs can construct and test new components and new specifications in a matter of minutes or hours, as opposed to days and weeks. Additionally, the time and cost

savings in part fabrication and physical testing quickly cover the initial setup cost of the simulation software and associated data acquisition hardware.

Extensive use of statistical modeling techniques can further increase efficiency in engine development time and cost. By employing statistical Experimental Design, one can collect data in a manner that permits construction of comprehensive statistical models of the physical engine. By using the Response Surface Analysis Method of model optimization these statistical models may be optimized in terms of all included variables simultaneously. Such statistical modeling drastically reduces development time by determining mathematical relationships between different variables using acquired data, and then mathematically finding the optimum settings for that system.

It is not the purpose of this paper to provide an in-depth study of Ricardo's WAVE software or Response Surface Methodology. Such in-depth studies on RSM and MRSM (RSM with multiple responses) and their use in engine development have already been conduced by Dvorak and Hoekstra (1, 2). Additionally, the work of Jemail (3) provides a detailed analysis of the construction of a WAVE simulation using dynamometer data. The intent of this paper is to utilize these two tools to examine the relationships between intake runner upstream diameters and plenum insert dimensions in a NASCAR restrictor plate intake manifold.

CHAPTER TWO: METHODOLOGY

The initial phase of the project involved construction of the WAVE simulation of the baseline engine. Construction of such a model requires substantial data acquired from a running engine, in addition to physical dimensional data. Such data as crank-angle resolved combustion data at each RPM step for each engine cylinder, oxygen sensor data, exhaust temperature data, intake manifold air charge temperature data, wall temperature data for the entire intake and exhaust system, and valve motion data.

Initial data was collected at Evernham Motorsports. Flow data for the cylinder heads, intake manifold, manifold insert, restrictor plate, carburetor, and exhaust headers was obtained on EMS' SuperFlow 1020 computerized flow bench. Combustion data for the initial setup was acquired on EMS' dynamometer. Ideal valve motion and intake manifold geometry were also obtained through EMS. While not all data required was available through EMS, a rough initial model was constructed based on the supplied data.

After construction of the initial model was completed, another experiment was conducted at Arrington Racing Engines on their dynamometer. Combustion data was obtained through an MTS combustion data acquisition system. In-cylinder pressure was measured using piezo-crystal transducers integrated into the spark plugs. All exhaust system wall temperatures were measured using thermocouples attached to the outer walls of the header system, while EGTs were measured with thermocouples mounted in adapter plates that were sandwiched between the cylinder heads and header primaries. Intake manifold wall temperatures were measured with thermocouples bonded to the interior walls of the intake manifold. Oxygen sensor readings were taken using a single wide band oxygen sensor mounted downstream of the second merge

collector on the driver's side header. In addition to the above data, oil pressure, temperature, air flow, fuel flow, fuel temperature, and fuel pressure were all measured through the dynamometer's built in data acquisition system.

In addition to the dynamometer acquired data, the cylinder heads were flowed on ARE's Super Flow 1020 flow bench, and a coordinate measuring machine was used to obtain detailed area progression profiles for the intake manifold. Detailed area progression data for the intake port of the cylinder heads was obtained from a Catia model of the port. Intake manifold, plenum insert, carburetor, and restrictor plate flow data obtained at EMS was retained for use in the new model. In place of the ideal valve motion supplied by EMS, Dodge Motorsports provided a full set of Spintron valve motion traces for use with the model, thus allowing the full effects of the valvetrain dynamics to be modeled with one set of parameters.

Upon initial setup of the new model, given the dimensions and combustion data acquired through ARE, validation of the baseline model was conducted. During the dynamometer testing at ARE, three different engine configurations were tested, thus providing an A, B, and C test for use when validating the simulation against the real world data. All three tests used ARE engine block number 179, with the baseline setup built on September 9, 2003. The A test was the Dodge Motorsports restrictor plate engine configuration for the first part of the 2003 season. For test B, the size of the restrictor plate was changed to reflect NASCAR's move from the 7/8" diameter restrictor plate to the 29/32" diameter plate. Test C removed four inches of header length between the first and second merge collectors while also retaining the larger restrictor plate. An additional test D was conducted on the dynamometer, but the change in engine output was small compared to the B and C tests, and was therefore not used for validation purposes. Once validated, the simulation of Test C was used for the intake manifold optimization tests due

to its greater output on both the dynamometer and on the computer.

Much is known and published about intake manifold runner dynamics, specifically wave propagation and the effect of the shape of the open end of the runner. Brandstetter (4) identified significant features of inlet system tuning. However, little has been published in regards to runner-to-runner interactions in common-plenum manifolds (as opposed to individual runner manifolds, or velocity stacks). Though Tabaczynski (5) touches briefly on such interactions in reference to a Jaguar racing engine, no qualitative discussion ensues. Additionally, no publications have been found regarding the flow dynamics in the uniquely shaped NASCAR restrictor plate manifold plenum inserts. For a schematic of the current manifold design, refer to Figure 1. The insert creates what is referred to as the "secondary plenum": an additional plenum volume bounded by the outer surfaces of the insert and the inner walls of the manifold's plenum. Experimentation on running engines has shown dramatic gains in IMEP and dramatic reductions in cyclic IMEP variability with the inclusion of such inserts on these engines.

Two main theories exist regarding the function of such inserts. The first theory views the secondary plenum volume as a damping volume, where the pressure waves reflecting off of the back side of the intake valve are trapped and dampened. Such a dynamic would dramatically reduce the number and magnitude of reflection waves that could cross the plenum and cause interference in other runners. It is such wave interference, both constructive and destructive, which greatly increases cyclic variability of cylinder charging. This theory, however, is not consistent with intake manifold time-pressure data observed at Arrington Engines on the test engine. A pressure transducer placed in the secondary plenum volume showed sixteen significant wave fronts per engine cycle, rather than the eight significant fronts that would be expected if the secondary plenum were acting as a damper. This does not necessarily disprove the theory,

however, as no pressure data was observed in the main plenum on the test engine. It is possible the secondary plenum does damp the waves relative to the main plenum.

The second theory views this secondary volume as a reservoir of air from which the cylinder can draw an air charge under such heavily restricted breathing conditions. This theory is supported by the engine's response to runner volume. According to Tabaczynski's (5) work on intake system tuning, maximum volumetric efficiency is achieved with a mean inlet mach (MIM) number of 0.5. However, given the heavily restricted inlet flow, the most powerful NASCAR restrictor plate engines have shown power gains with runner diameters sufficiently large that the MIM is closer to 0.3, rather than 0.5, indicating the presence of some other governing dynamic in the inlet system.

The goal of the RSM analysis is to analytically predict the dimensions of the upstream runner diameter and insert to provide the maximum brake horsepower. The results of this analysis should lead to a further understanding of the dynamics at the insert-to-runner junction, as well as the secondary volume's main role in the fluid flow in the manifold. In order to capture as many geometric entities as possible while retaining a manageable matrix, the following assumptions were made:

- Intake runner geometry for cylinders 1 and 8 are symmetric.
- Intake runner geometry for cylinders 2 and 7 are symmetric.
- Intake runner geometry for cylinders 3, 4, 5 and 6 are symmetric.
- Intake runner area progression is linear from upstream end of runner to cylinder head mating flange.

Additionally, the variable used to quantify the geometry of the insert at the runner to plenum

interface is referred to as the “window”, which is the area between the bottom of the intake runner and the insert “finger” which extends from the inner wall of the insert into the runner’s upstream end (See Figure 1). The area above the “finger” was calculated by subtracting the area of the window from the area of the runner at that point. The cross sectional area of the intake runner at the cylinder head flange is held constant, and for cylinders 1, 2, 7 and 8, where the runner’s geometry is divided into 2 lengths for each cylinder in the WAVE model, the midpoint area is the average of the upstream and downstream areas, providing a linearly decreasing area progression from plenum to cylinder head.

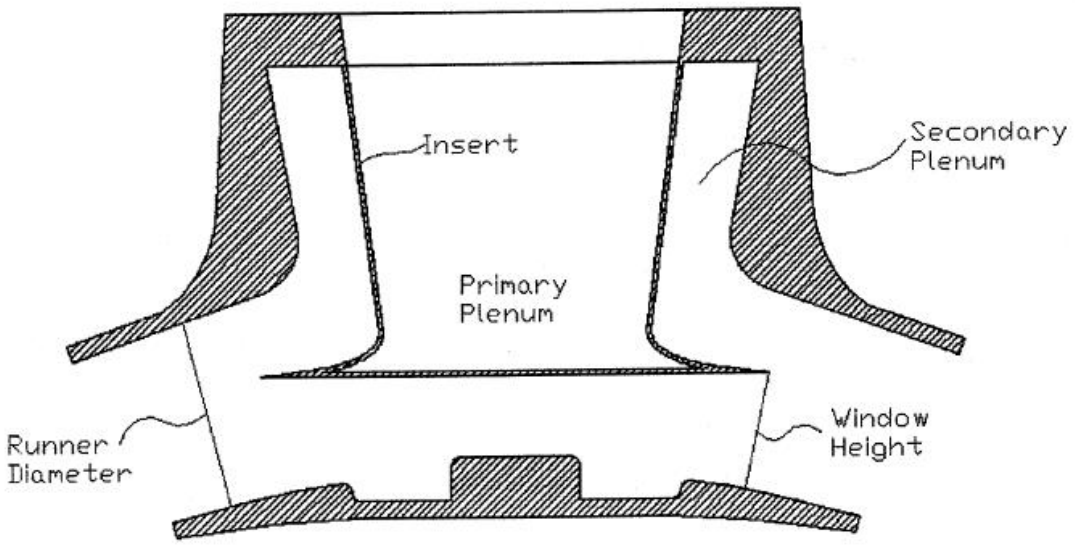

Figure 1: General shape of NASCAR restrictor plate manifold and insert

Typically, the first step in constructing a statistical model is the screening test, in which a 2 level factorial design is created and executed in an attempt to determine which potential main

effects are statistically significant. By screening the main effects with this smaller design, one can save significant time and cost in experimentation by excluding effects which are determined to be insignificant. In this case, however, experience indicates that all six factors in the intended design are significant to some degree, and the presence of the simulation makes the time and monetary cost to perform the extra runs negligible. Additionally, because little is truly understood regarding the dynamics of the restrictor plate manifold and insert system, any findings in the second order design are of interest.

Therefore, the design created and executed in the WAVE software was a six- factor central composite design, or CCD. The CCD design has many benefits in this particular application. In order to help visualize the design space, one can think of a three factor CCD in three dimensions. A CCD obtains data at the corners, center, center of the edges, and center of the faces of the cube. Additionally, points radial to the center of the cube outside of the cube's dimensions are obtained, such that they and the corner points of the cube define a curved volume. These radial points, referred to as axial points, are defined by a scalar α. This scalar is the ratio of the axial point's distance from the design center to distance from the cubic face to the design center.. If $\alpha = 4\sqrt{F}$, where F = number of factorial points, then the volume enclosed by the axial points and corner points is spherical. Such a shape results in a design that is said to be rotatable. A rotatable design is preferred due to the constant scaled prediction variance throughout the design space. Because the optimum setting's location in the design space is unknown at the commencement of the experiment, a constant scaled prediction variance is essential to ensuring that the mathematical optimum settings are an accurate prediction of the response (6). In the case of this 6 factor design, this yields an $\alpha = 2.828$. Using the existing manifold dimensions as the center of the design, the +/- 1 boundaries are set to +/- 0.200"

equivalent diameter. These values are based on the available material thickness in the existing manifold's casting surrounding the current runners. Therefore, the majority of the design takes place within the physical constraints of the existing casting. As with any experiment designed to examine existing theory, it is also necessary to examine regions outside of the current constraints in a search for theoretical gains. This factor, combined with the $\alpha = 2.828$ results in runner diameters at the axial points outside of the physical casting.

The resulting six-factor CCD matrix yields 76 experimental runs in addition to the center runs. The center runs are intended to provide two critical features to the design space. The first is to provide an estimate of curvature to the second order design. The second feature is to provide an estimate of variance in the design space. Combining a sufficient number of center runs with a rotatable design, the experimenter obtains a good understanding of the prediction variance in the entire design region. However, a computer simulation such as WAVE affects the number of center runs necessary to achieve this prediction variance. The WAVE simulation can be configured to begin its iterative calculations at two different locations. The first choice is to use the final boundary conditions from the previous experiment as the initial boundary conditions for the next. While this theoretically improves processing time, it eliminates the essential independence of the runs from one another. The second choice, and the one chosen for this experiment, uses a set of global initial conditions for every run in the entire matrix. This allows the experimental runs to be conducted truly independently from one another, however, yields an identical response for every replicate of an experimental run. In short, the replicate variance in the design space = 0. Therefore, the number of center runs for the experiment is 1, to provide for

curvature in the design. Any additional center runs would provide identical responses, and are therefore wasteful.

Upon completion of the 77 run matrix, the WAVE model was modified for the experimental runs. Each experimental run requires seven cases in WAVE, as each experiment must be conducted at each of the seven RPM steps measured on the dynamometer. The resulting 539 cases in WAVE were broken down between three copies of the WAVE model. The computers available for running the simulations begin to slow drastically as the number of cases exceeds 250, requiring the multiple copies of the simulation. Total simulation time for the 77 run matrix is approximately 15 hours.

The output from the 539 total cases was broken down by experimental run, at which time the average brake MEP was calculated. Using the average BMEP for each experimental run, the six-factor matrix was analyzed using Minitab v13. Using the data to define a full second order relationship, terms were eliminated one by one based on the highest remaining p value in the set. This iteration continued until the mean squared error of the system was minimized.

The relationship resulting from screening the second order design contains numerous terms with p values greater than the 0.1 significance level intended. This indicates correlation between the various terms that is not captured in this experiment. Despite this fact, the relationship appears to provide a reasonably good predictor of the simulation's response, due to the MSE of 0.1114 and an adjusted R-squared value of 98.3%. Given this, the system was analyzed for a point of maximum response using the stationary point method. This method uses matrix algebra to find the point where all of the partial derivatives of the defining relation are equal to 0. This location can be a maximum, minimum, or saddle point. Additionally, it is possible for the point to be a local maximum or minimum, where the system's global peak values

lie outside the design space.

The stationary point analysis yielded a stationary point of x1 = -117.2”, x2 = -239.1”, x3 = -151.6”, x4 = 5.4”, x5 = 1.2”, and x6 = 7.0”. Clearly the stationary point for this system lies far outside the boundaries of the design space, not to mention physical possibility. Therefore, no mathematical maximum, minimum, or saddle point within the design space exists.

CHAPTER THREE: RESULTS

Because there is no optimum point within the design space, the shape of the relationship within the design region must be examined in order to determine the direction in which the optimum settings reside. Using Minitab 13, there are two methods for examining the shape of the relationship in the design region. The first method is by using the built-in response optimizer function. While this function rarely produces the optimum point in the relationship, even when a stationary point exists, it is fairly good at approximating the shape of the region. Figure 2 shows the response optimizer's interface. From this figure, it is clear that the relationship is near an optimum in terms of runner equivalent diameter, but still desires a larger window area. Table 1 shows the values determined using the response optimizer.

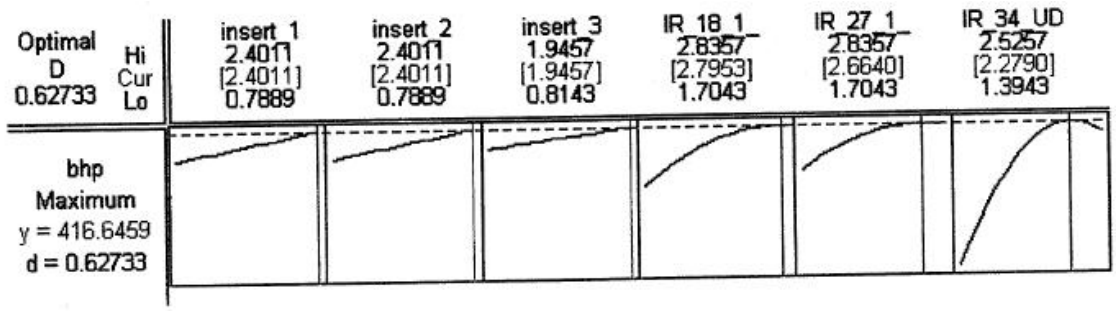

Figure 2: Minitab 13 Response Optimizer interface

Table 1

Response Optimizer Function Values

Variable	Method A	B	C
Window Equiv. Diam, Runners 1/8	2.401”	2.401”	1.880”
Window Equiv. Diam, Runners 2/7	2.401”	2.401”	1.880”
Window Equiv. Diam, Center Runners	1.945”	1.945”	1.580”
Upstream Equiv. Diam, Runners 1/8	2.832”	2.795”	2.470”
Upstream Equiv. Diam, Runners 2/7	2.820”	2.650”	2.470”
Upstream Equiv. Diam, Center Runners	2.321”	2.279”	2.160”
Predicted Response, BHP	416.54	416.65	413.87
Simulated Response, WAVE, BHP	415.25	415.36	413.52

Prediction Method: A = Minitab computed optimum response, B = author-forced optimum response within Minitab, C = best predictor from CCD Matrix

The Minitab Response Optimizer will predict an optimum location based on user specified criteria. These criteria are:

- Desire for a maximum, minimum or target response
- Minimum, maximum and target response values
- Relative importance of each main effect in the solution to the experimenter

Column A in Table 1 is the Minitab optimized solution based on a minimum acceptable response of 411 BHP, attempting to maximize the BHP, with a target value of 420 BHP. These values were chosen based on experience with the optimizer function and its interface with the data. Additionally, the experimenter may force the settings for the main effects based on the graphs

shown in Figure 2. Column B of Table 1 shows those forced settings. These two optimum settings are then compared to Column C, which illustrates the single highest output settings from the 77 run matrix. From this comparison, the advantages of the RSM relationship are clear, despite the lack of a mathematically optimized solution within the design space.

Another accepted method of determining the shape of the relationship in the design region is through graphical analysis of contour plots of the response versus two main effect variables. While this can be a useful tool, it must be noted that one major drawback to this method in Minitab is the inability to force the values of the other main effects to any value other than that of the center point of the design. Therefore, it is quite possible for interactions to be lost in the graphical analysis. The contour plot shown in Figure 3 compares the variables of interest in runners 1 and 8 to the BHP response of the system. From this contour plot, it is clear that the system's peak output should occur when the insert's equivalent diameter is approximately 1.700", and the upstream equivalent diameter is approximately 2.750". However, this contrasts with the response optimizer's plots, which indicate that the equivalent window diameter must be maximized to obtain peak performance.

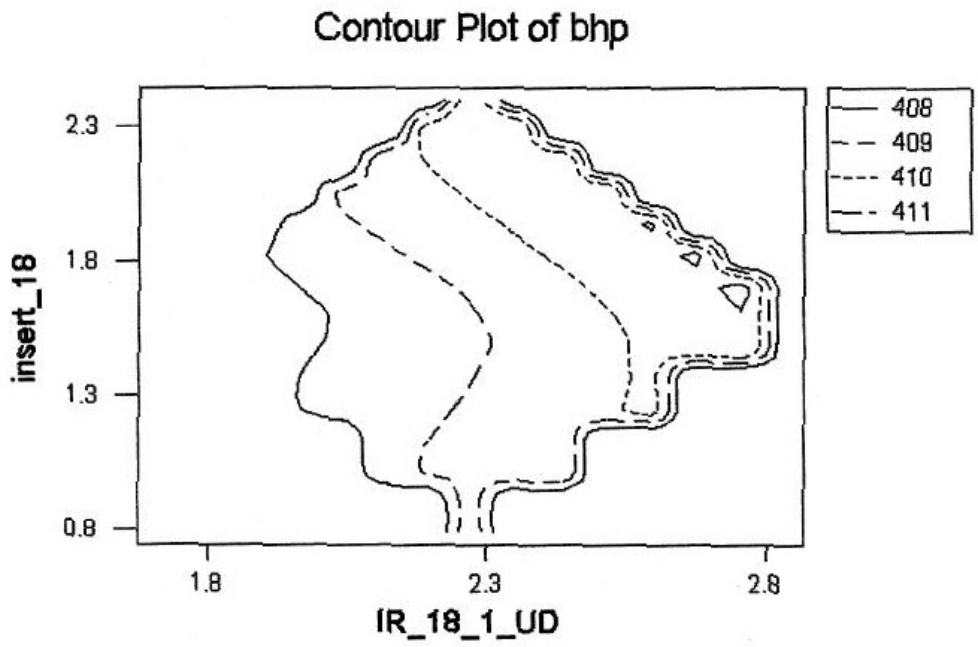

Figure 3: Contour Plot of bhp

The contour plot in Figure 3 is included to show the conflict between the two analytical methods. For the complete set of contour plots, refer to Appendix A.

While analyzing the data from the RSM model and the simulation, discontinuities between dynamometer experience and model results began to appear. The main discontinuity lies in equivalent insert opening diameter, that is, the area between the insert's horizontal flange and the roof of the intake port. This area represents the opening of the secondary plenum into the intake runner. Dynamometer experience indicates the necessity for a large opening to the insert; however, the model predictions show a trend towards a smaller secondary plenum opening and a larger window area. This inconsistency leads to questions about the accuracy of the simulation.

While the simulation's global performance is close to that of the tested engine, does that necessarily mean that simulation performance in the middle of the model is representative of the tested engine?

The authors believe the model is not representative of the running engine in its prediction of flow dynamics at the insert's interface with the runners. This belief is based on the principles of compressible fluid flow in a curved duct. Especially in high speed flow, such as that seen in the intake runner of an engine at high engine speed (in this case between 6000 and 7200 RPM), the majority of air and fluid flow is present along the outside radius of the curved pipe. This is due to the fluid's inertia, and the lower path of resistance along the outer wall of the runner. The clearest demonstration of this principle can be conducted on a flow bench with a pressure probe. At high airflow velocities through a port, the lowest pressures (which represent the highest air velocities, as per Bernoulli's theorem) are measured along the outside radius of the port. This phenomena occurs both on flow towards the cylinder, and returning from the cylinder. Such a compressible flow phenomena would force a disproportionate mass of air and fuel to the roof of the intake runner. Given the geometry of the plenum insert, this would result in a comparably disproportionate mass of air and fuel entering the secondary plenum. However, the WAVE simulation software models one-dimensional compressible two- phase fluid flow. Neglecting wall friction and boundary layer phenomena, WAVE assumes a pressure gradient across the duct cross-section of zero. While this may be an adequate assumption in modeling traditional intake runners and manifolds, the authors believe that this simplified view is inadequate for modeling the three-dimensional aspects of current NASCAR restrictor plate intake manifold insert dynamics.

An investigation of the intake system tuning by Tabaczynski (5) reveals the importance

of runner diameter and length tuning to provide the desired torque curve. The standard method for this type of tuning is the Helmholtz resonator method. While Tabaczynski showed the importance of resonance tuning intake runners to the engine, Selamet, Dickey, and Radavich (7) compared the resonant frequencies of a series of test pipes using experimental, one-dimensional theoretical, and three-dimensional analytical methods. Despite the fact that the test pipes were straight, uniform cross-section pieces, the three-dimensional analytical method clearly showed its superiority to the one-dimensional approach in finding the resonant frequency of the pipe.

Another area of concern for the authors regarding simulation accuracy lies in fuel distribution throughout the engine. Comparisons between the WAVE simulation and ARE dynamometer data were conducted on individual cylinder output. The relative performance of each cylinder with respect to the rest of the engine was not consistent between the WAVE simulation and the ARE dynamometer data. Extensive work on identifying possible errors in simulation coding and/or modeling was conducted. After three months of additional development on the model, as well as information obtained from Ricardo on the base program coding, it is the authors' conclusion that primary cause of this discrepancy lies in how WAVE handles fuel distribution. Once introduced into the engine, WAVE assumes perfect mixing of air and fuel. Thus, the air/fuel ratio selected by the user as an engine average actually becomes the specific AFR for each individual cylinder; relative cylinder performance is determined solely by airflow distribution, and cannot be affected by fuel distribution issues. Additionally, the software assumes the fuel never separates from the airstream, and therefore cannot puddle or pool in the intake tract. Experience with these engines indicates that significant fuel distribution and fuel separation problems exist in the physical engine.

CHAPTER FOUR: FINDINGS

In the WAVE simulation, we try to model the wave propagation and flow through a non-uniform cross-section, curved pipe using one-dimensional compressible flow techniques. In an attempt to determine the feasibility of collecting max flux data at the various locations in the intake runner and forcing the one-dimensional model to represent the three-dimensional effects, an experiment was conducted in WAVE forcing the reverse-flow discharge coefficient of the window to values of 1, 0.8, and 0.6. As expected, as the reverse flow DC is reduced, the mass flux through the secondary plenum opening increases, with a maximum delta of approximately 150 g/s during the compression stroke. An inspection of the graphs in Appendix B reveals the maximum delta in max flux across the secondary plenum opening during the time following IVC, reducing to a delta of nearly zero at the time of IVO. This results in nearly identical mass flux from the secondary plenum into the runner at all DCs examined. This also strongly correlates to the nearly identical BHP values for all DCs examined. This correlation combined with the presence of 4 distinct pressure waves per cycle below 6600 RPM, and 3 pressure waves per cycle at 6600 RPM and up tends to disprove the theory that the secondary plenum acts solely as a surge suppressor, dissipating the reflection and reversion pulses. It is the author's contention that the plenum insert serves three distinct functions.

First, in the three-dimensional case, the insert serves to prevent the reversion pulses from entering the main plenum and entering other runners, thereby reducing wave interference and cyclic variability in cylinder filling. Second, by "catching" these reversion pulses and reflecting them back down the runner, the insert appears to be partially transforming the intake runner into

a closed-ended pipe, where the damping of the wave energy arises mainly from heat and wall friction losses. This idea is supported by the pressure transducer data observed on the test engine showing sixteen distinct wave fronts in the secondary plenum volume, indicating relatively poor damping of the wave fronts. Third, the secondary plenum provides a reservoir of air for the cylinder to draw from during the intake stroke. It is also the author's contention that, given these observations and hypotheses, the WAVE simulation does not currently represent the full real-world dynamic of the plenum insert, but does show an indication of the wave propagation within this area of the engine. This contention is based on the conflict between the model's desire for a larger and larger window, reducing the area for the secondary plenum opening, with the experimental data showing the need for a larger secondary plenum opening and smaller window. Experimental tests with the smaller windows support the theory of the wave "catching and reflecting" properties of the insert and indicate that the reduction of cyclic variability under heavily throttled conditions outweighs the importance of fresh air entering the runner through the window. However, wave propagation data obtained during the discharge coefficient sensitivity analysis agree with observations made on the test engine. While the boundary conditions within the model appear to be flawed, the general trend appears accurate.

To this point, there has been little discussion regarding the details of the model verification process. The RPM range of interest for this model is 6000–7200 RPM. However, the engine makes peak power in the 6600-6800 RPM range, therefore it is most critical for the simulation to be accurate in this region. WAVE uses the Chenn-Flynn friction correlation model, which is:

FMEP = ACF + BCF*Pmax + CCF * MPS + QCF * MPS^2

A major limitation to this friction correlation is it's inability to model higher order polynomials.

The MTS-measured friction curve is shown in Figure 4. It is apparent that the Chenn-Flynn friction correlation can not accurately represent the MTS-measured curve through the entire 6000-7200 RPM range. However, note the curve's nearly linear behavior from 6200-6800 RPM. In the interest of providing the best overall prediction in the area of interest, the friction correlation specified in WAVE was designed to fit this linear region.

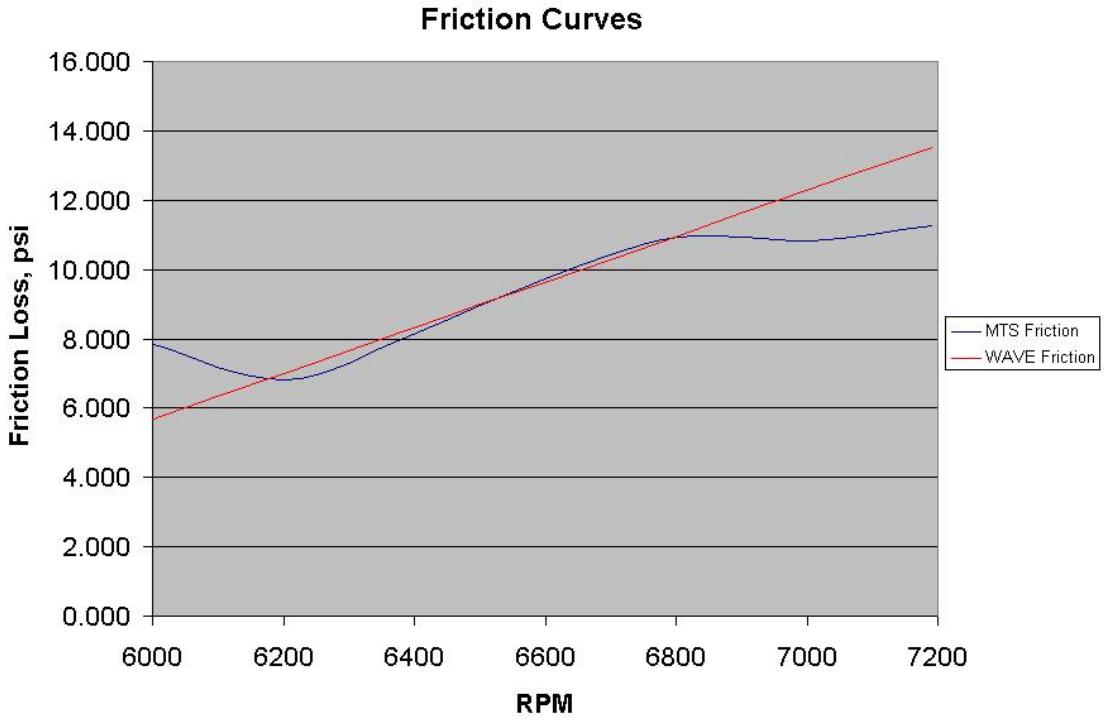

Figure 4: Friction correlation and MTS dynamometer friction curve

In addition to friction curve fitting, substantial efforts were made to reduce the pumping losses in the model. The WAVE simulation predicts excessive pumping losses when compared to the MTS dynamometer data. When compared to the dynamometer data, the WAVE

simulation accurately predicts BMEP and FMEP to within a 3% error from 6200-7000 RPM. However, due to the excessive pumping work, PMEP and IMEP are high, while airflow, fuel flow, and BSFC are low. Figure 5 contains the critical values from both the MTS and WAVE outputs.

	6000		6200		6400		6600		6800		7000		7200	
	EXP	WAVE	EXP	WAVE	EXP	WAVE	EXP	WAVE	EXP	WAVE	EXP	WAVE	EXP	WAVE
Actual RPM	5997	5997	6201	6201	6399	6399	6604	6604	6804	6804	7005	7005	7192	7192
FMEP	7.869	5.649	6.827	6.997	8.142	8.306	9.773	9.662	10.917	10.984	10.823	12.313	11.265	13.549
NMEP.EA	159.327	165.080	155.087	160.509	152.853	156.174	150.662	150.828	147.600	147.590	142.984	143.596	139.558	138.888
PMEP.EA	-3.353	-8.929	-3.896	-9.253	-4.657	-9.657	-5.557	-10.460	-6.372	-11.242	-6.964	-12.075	-7.589	-12.821
IMEP.EA	162.680	174.009	158.984	169.762	157.510	165.831	156.219	161.288	153.972	158.833	149.947	155.671	147.147	151.708
BMEP.EA	151.458	159.431	148.261	153.511	144.711	147.868	140.890	141.167	136.683	136.606	132.161	131.283	128.293	125.338
Air Flow (kg/hr)	988.740	942.860	999.450	952.598	1016.140	960.585	1024.350	967.758	1032.010	975.666	1035.230	982.984	1045.490	987.060
Fuel Flow (kg/hr)	73.160	70.890	73.350	69.540	75.750	70.116	75.930	75.017	75.160	72.274	77.200	72.814	77.700	71.018
BSFC	0.390	0.362	0.390	0.357	0.400	0.362	0.400	0.393	0.400	0.378	0.410	0.386	0.410	0.385
BHP	410.200	431.795	415.200	429.904	418.200	427.321	420.200	421.026	420.000	419.763	418.100	415.322	416.700	407.101
PisTemp	560.0	560.0	565.0	565.0	570.0	570.0	572.5	572.5	575.0	575.0	577.5	577.5	580.0	580.0
ChamTemp	593.0	593.0	596.5	596.5	600.0	600.0	602.5	602.5	605.0	605.0	607.5	607.5	610.0	610.0
CylTemp	310.0	310.0	314.0	314.0	318.0	318.0	321.5	321.5	325.0	325.0	328.0	328.0	331.0	331.0
% Error IMEP	-6.9639		-6.7795		-5.2826		-3.2447		-3.1566		-3.8169		-3.0997	
% Error BHP	-5.2644		-3.5414		-2.1811		-0.1965		0.0564		0.6643		2.3036	
% Error FMEP	28.2175		-2.5003		-2.0217		1.1351		-0.6150		-13.7652		-20.2798	
% Error PMEP	-166.2865		-137.4996		-107.3552		-88.2323		-76.4323		-73.4032		-68.9424	
% Error Air Flow	4.6402		4.6877		5.4672		5.5247		5.4597		5.0468		5.5888	
% Error Fuel Flow	3.1022		5.1947		7.4376		1.2026		3.8405		5.6820		8.6003	
% Error BSFC	7.1991		8.5670		9.5707		1.8032		5.3828		5.7352		6.2037	

Figure 5: Comparison of WAVE and experimental data

Due to discrepancies in the MTS supplied and WAVE calculated combustion events, extensive work in the area of combustion matching was conducted. An overlay of the physical and predicted combustion curves shows notable differences, as shown in Figure 6.

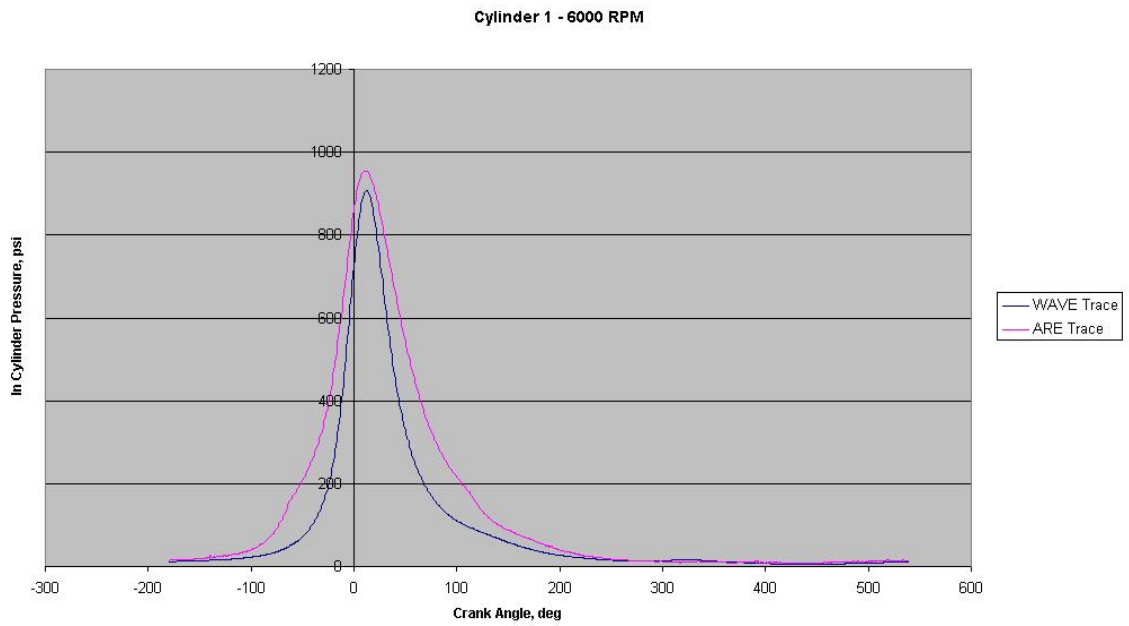

Figure 6: Comparison of WAVE and MTS (ARE) combustion traces

WAVE v5.2's heat release function is intended to help provide a more accurate heat release profile in the event a model's combustion curve does not closely match a Weibe relation. Attempts to utilize WAVE v5.2's heat release function to improve combustion, however, yielded negligible results.

CHAPTER FIVE: FUTURE RESEARCH

To better understand the wave propagation dynamics within the restrictor plate manifold and insert, data must be collected on the three-dimensional mass flux through the intake runners at different locations along the runner's length. Such data would provide boundary conditions for the modification of the current one-dimensional WAVE simulation to represent the three-dimensional flow. Such data would also be invaluable in the development of three-dimensional CFD models of two-phase fluid flow.

In addition, it should be noted that the RPM at which the number of waves across the secondary plenum entrance changed from four waves to three is also the RPM at which the B E1P is maximized. Inspection of the mass flux plots in Appendix B will show that 6600-6800 RPM appears to be the resonant frequency for the number 1 and 8 intake runners. Should it be determined that the insert were actually reflecting the reversion pulses rather than dissipating them, an investigation into the feasibility of tuning the distance from the insert's vertical wall to the intake valve could yield a manifold with better resonance tuning. On such a heavily throttled intake system, cyclic variability and resonance tuning become increasingly important.

Finally, given the differences in in-cylinder pressure profiles and pumping work, collecting another set of in-cylinder pressure data on an identical motor could provide a set of data with which to compare, hopefully identifying and correcting any systematic errors which may exist in the current set of data.

APPENDIX A:
MINITAB CONTOUR PLOTS

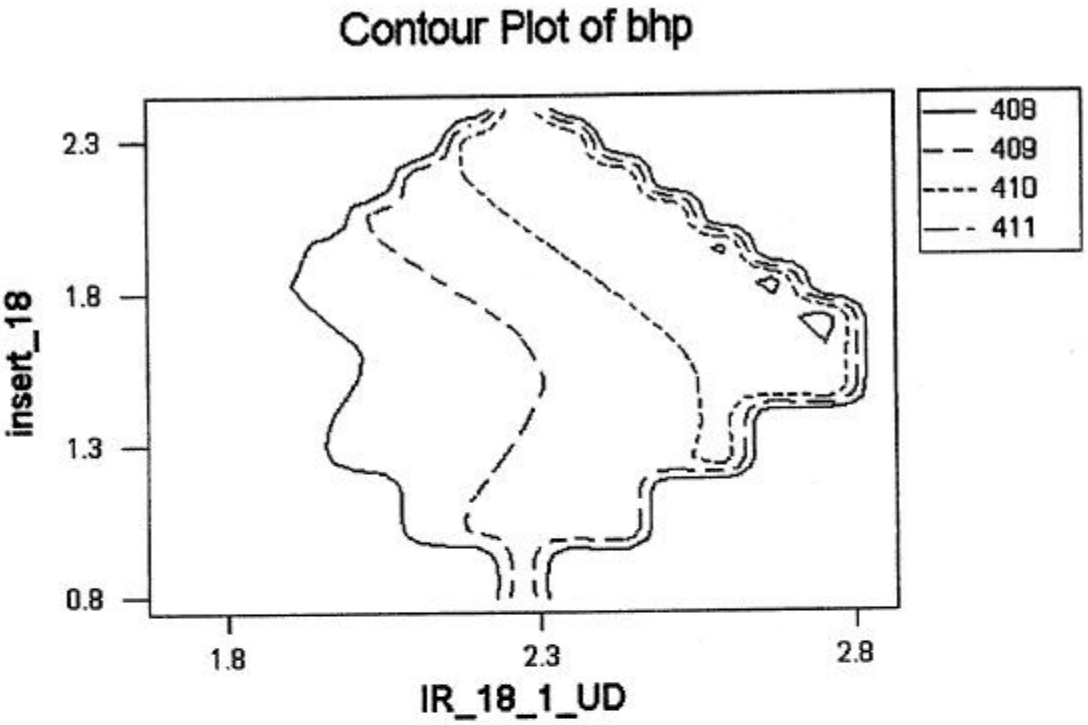
Contour Plot of bhp
408
409
410
411
insert_18
2.3
1.8
1.3
0.8
1.8
2.3
2.8
IR_18_1_UD

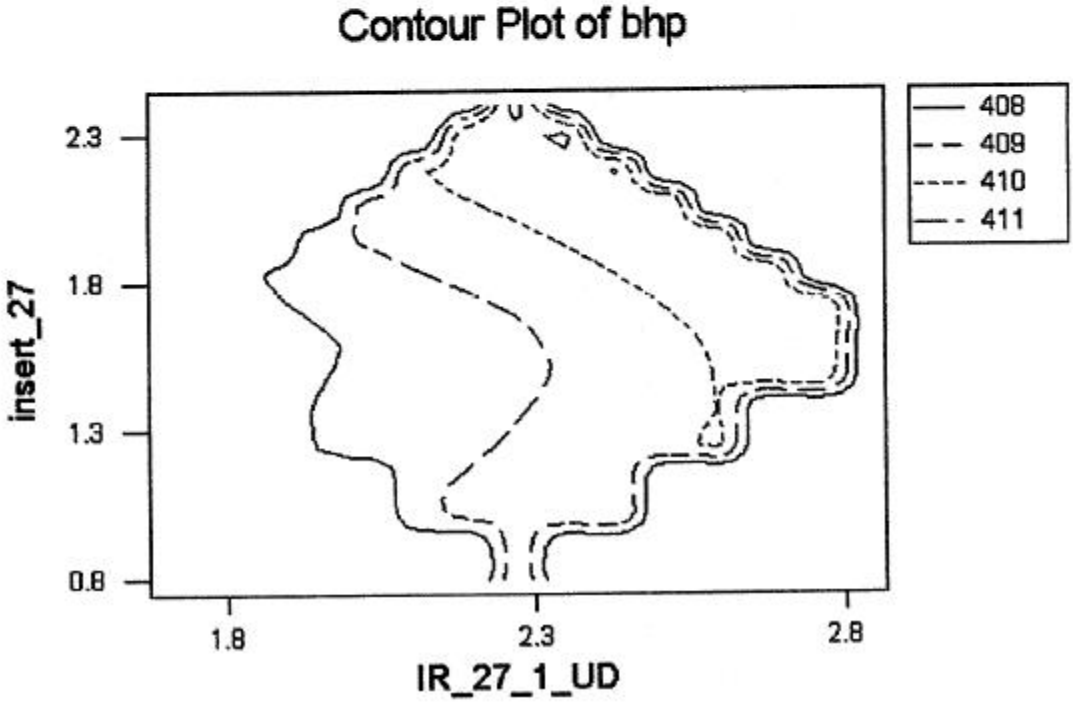
Contour Plot of bhp
408
409
410
411
insert_27
2.3
1.8
1.3
0.8
1.8
2.3
2.8
IR_27_1_UD

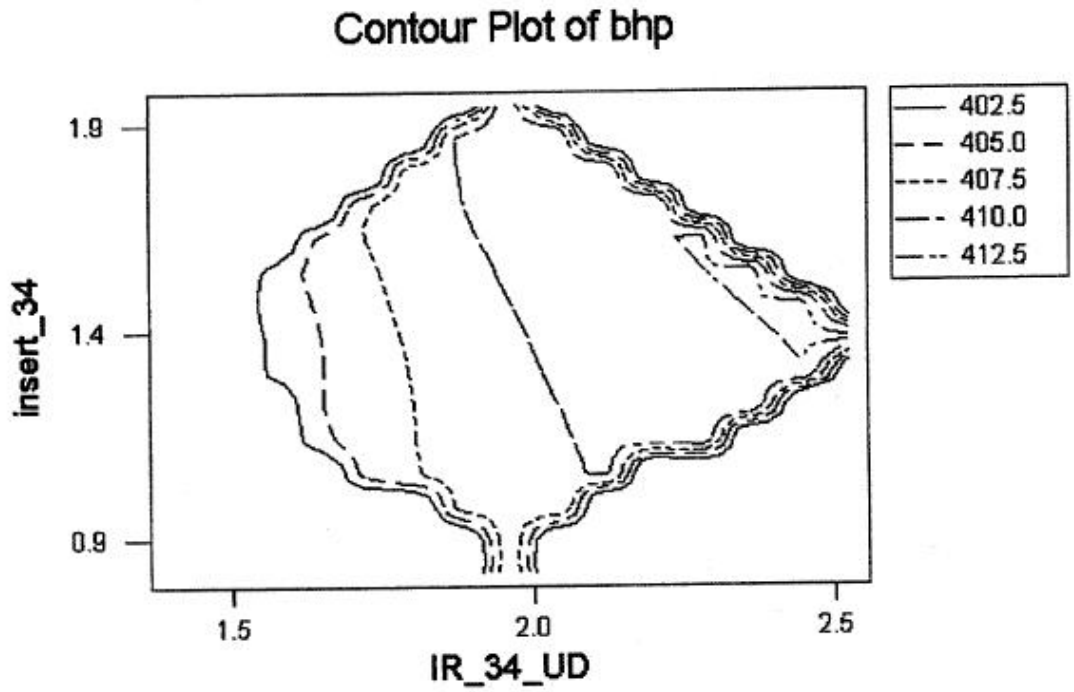
Contour Plot of bhp
402.5
405.0
407.5
410.0
412.5
1.9
1.4
0.9
insert_34
1.5
2.0
2.5
IR_34_UD

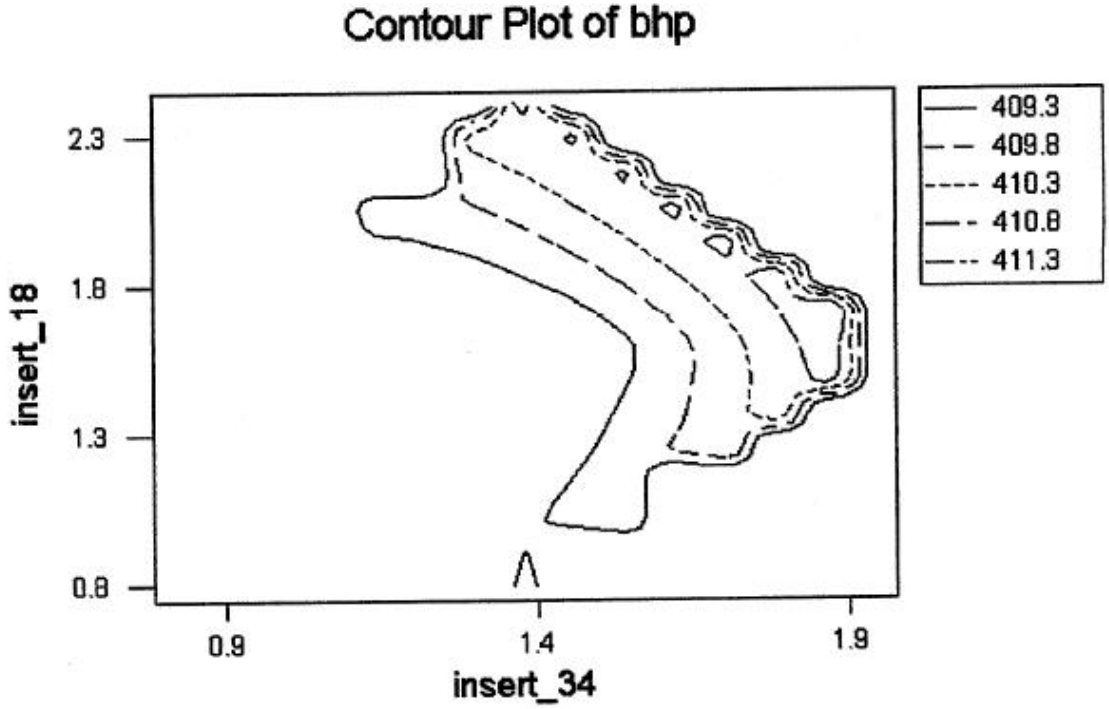
Contour Plot of bhp
409.3
409.8
410.3
410.8
411.3
2.3
1.8
1.3
0.8
insert_18
0.9
1.4
1.9
insert_34

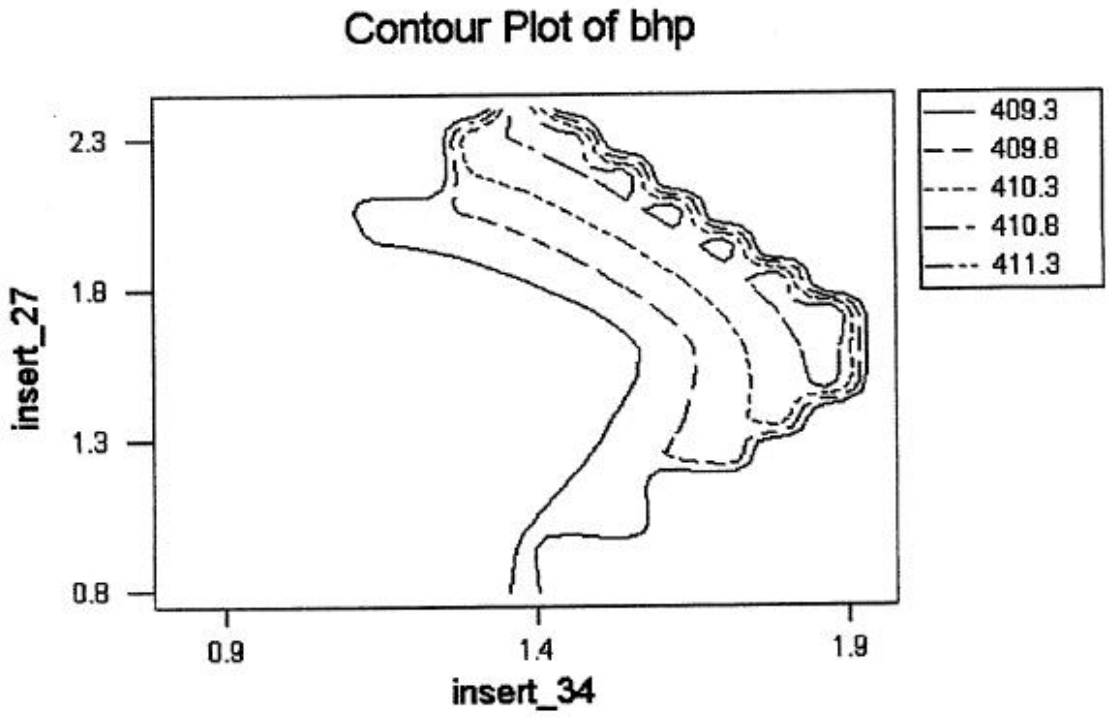
Contour Plot of bhp
409.3
409.8
410.3
410.8
411.3
2.3
1.8
1.3
0.8
insert_27
0.9
1.4
1.9
insert_34

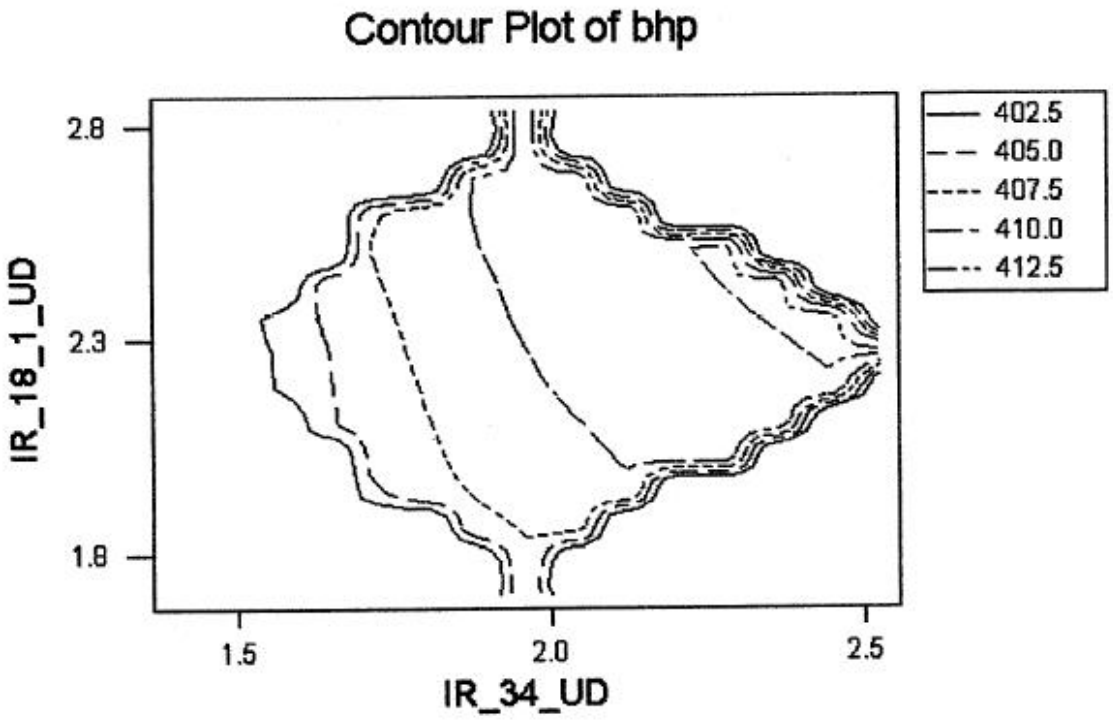
Contour Plot of bhp
402.5
405.0
407.5
410.0
412.5
2.8
2.3
1.8
IR_18_1_UD
1.5
2.0
2.5
IR_34_UD

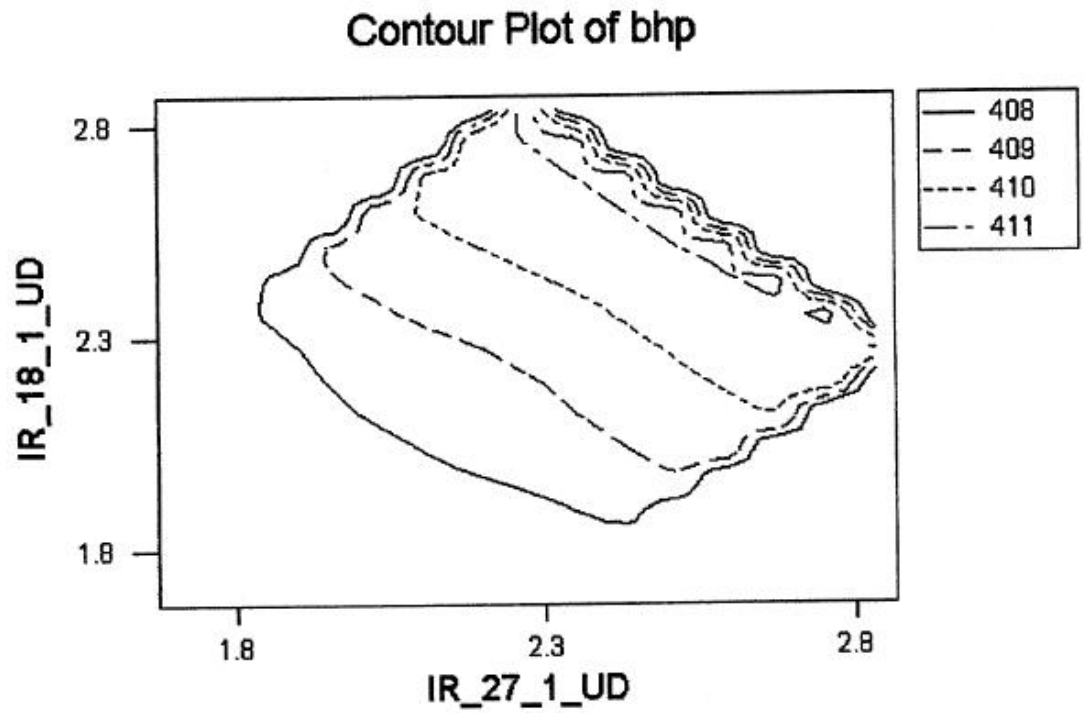
Contour Plot of bhp
408
409
410
411
2.8
2.3
1.8
IR_18_1_UD
1.8
2.3
2.8
IR_27_1_UD

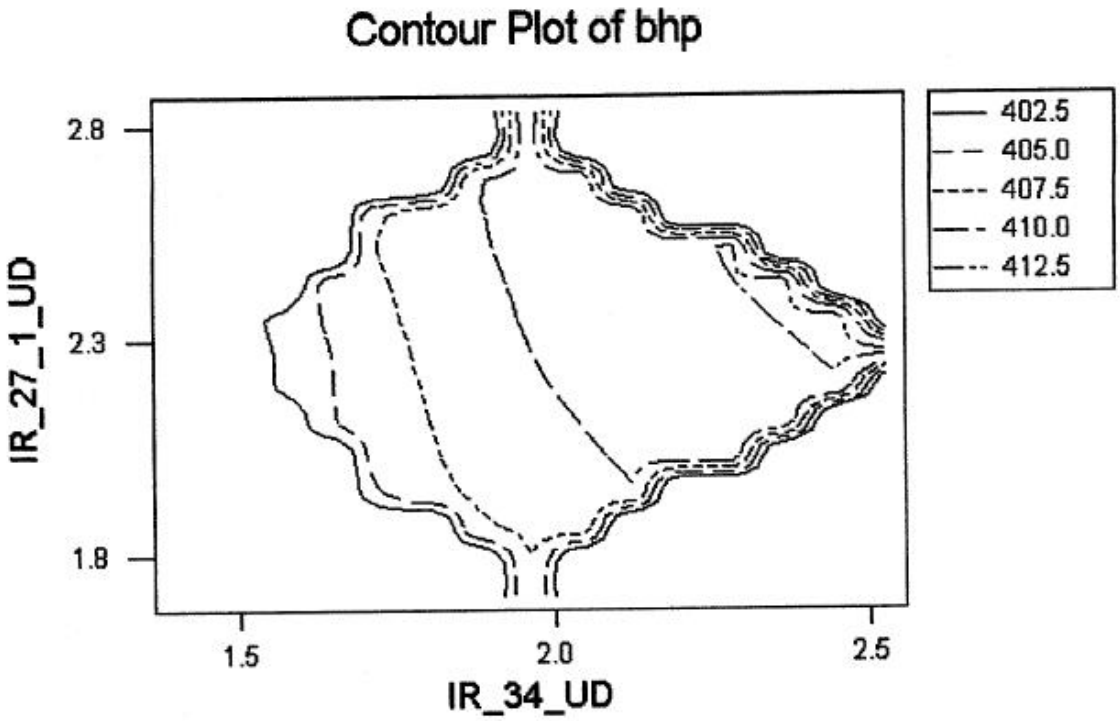
Contour Plot of bhp
402.5
405.0
407.5
410.0
412.5
2.8
2.3
1.8
IR_27_1_UD
1.5
2.0
2.5
IR_34_UD

APPENDIX B:
MASS FLUX PLOTS AT MANIFOLD INSERT

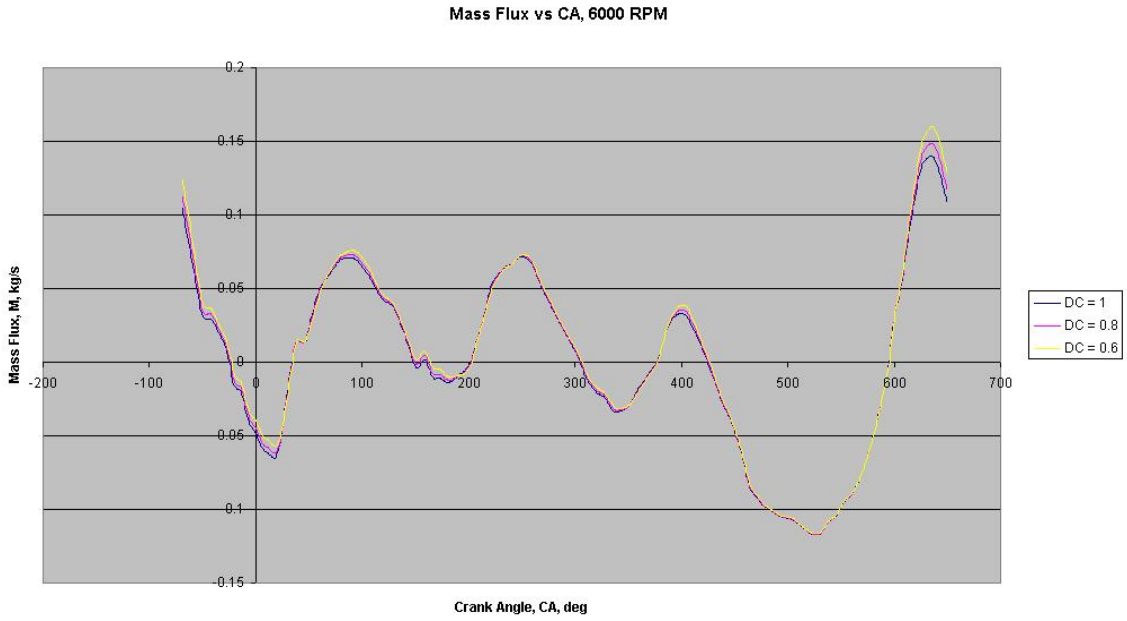
Mass Flux vs CA, 6000 RPM
Mass Flux, M, kg/s
0.2
0.15
0.1
0.05
0
0.05
0.1
-0.15
-200
-100
0
100
200
300
400
500
600
700
Crank Angle, CA, deg
DC = 1
DC = 0.8
DC = 0.6

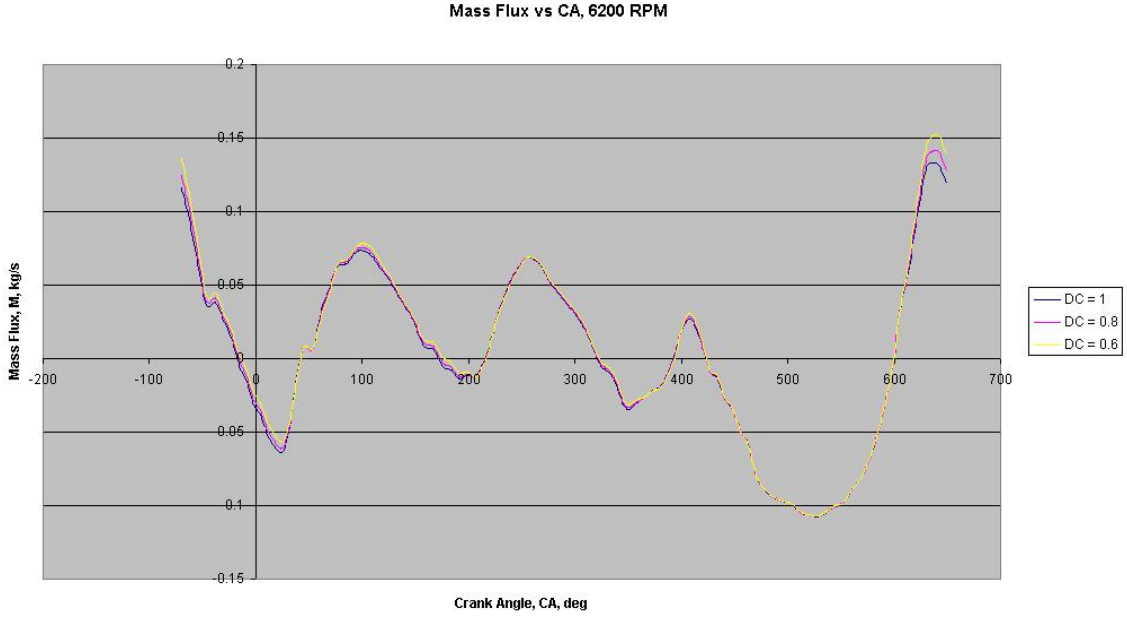
Mass Flux vs CA, 6200 RPM
Mass Flux, M, kg/s
0.2
0.15
0.1
0.05
0
0.05
0.1
-0.15
-200
-100
0
100
200
300
400
500
600
700
Crank Angle, CA, deg
DC = 1
DC = 0.8
DC = 0.6

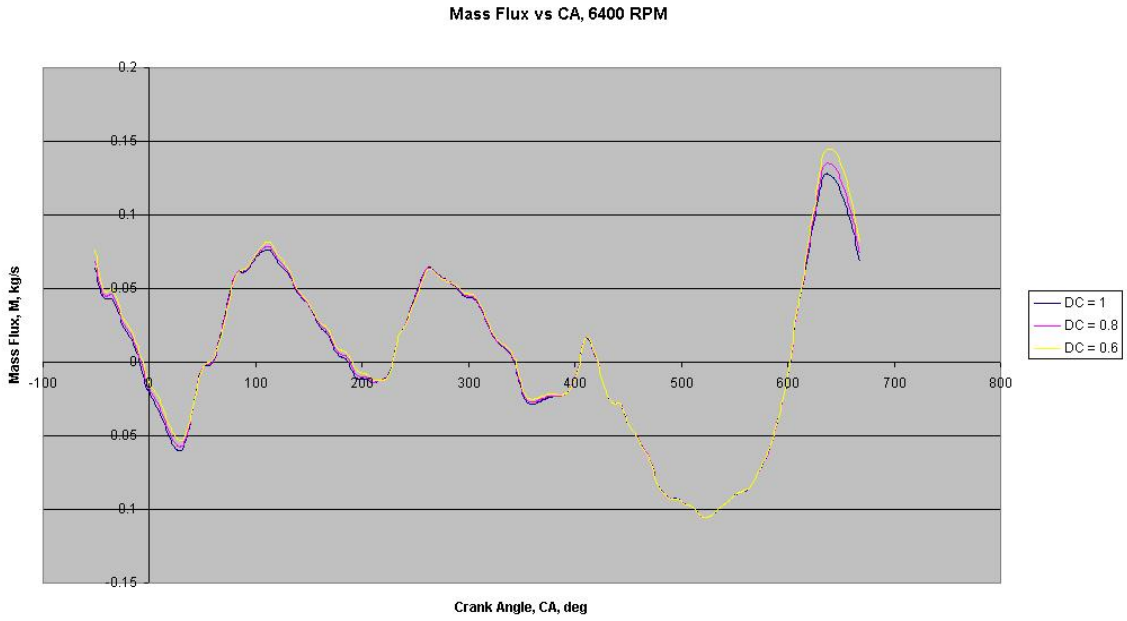
Mass Flux vs CA, 6400 RPM
Mass Flux, M, kg/s
0.2
0.15
0.1
0.05
0
0.05
0.1
-0.15
-100
0
100
200
300
400
500
600
700
800
Crank Angle, CA, deg
DC = 1
DC = 0.8
DC = 0.6

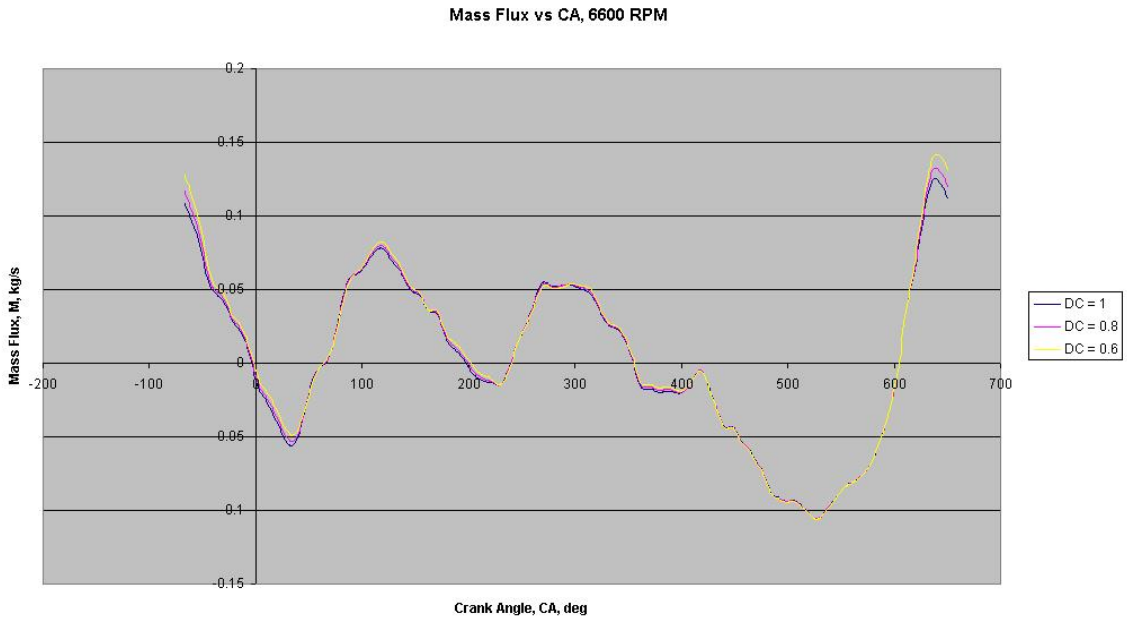
Mass Flux vs CA, 6600 RPM
Mass Flux, M, kg/s
0.2
0.15
0.1
0.05
0
0.05
0.1
-0.15
-200
-100
0
100
200
300
400
500
600
700
Crank Angle, CA, deg
DC = 1
DC = 0.8
DC = 0.6

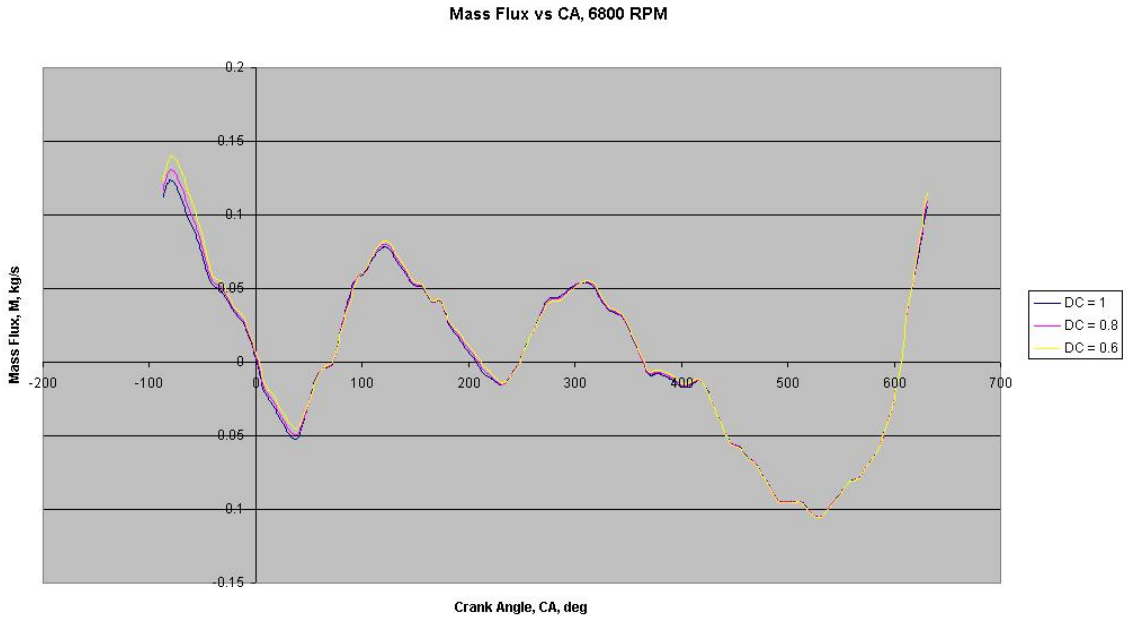
Mass Flux vs CA, 6800 RPM
Mass Flux, M, kg/s
0.2
0.15
0.1
0.05
0
0.05
0.1
0.15
-200
-100
0
100
200
300
400
500
600
700
Crank Angle, CA, deg
DC = 1
DC = 0.8
DC = 0.6

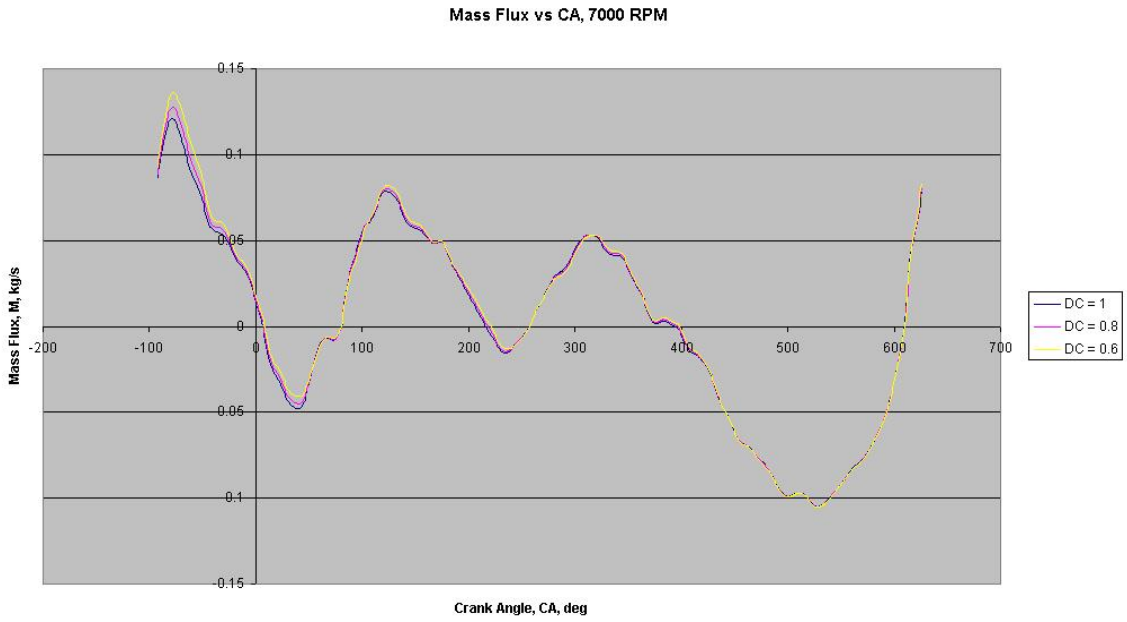
Mass Flux vs CA, 7000 RPM
Mass Flux, M, kg/s
0.15
0.1
0.05
0
0.05
0.1
0.15
-200
-100
0
100
200
300
400
500
600
700
Crank Angle, CA, deg
DC = 1
DC = 0.8
DC = 0.6

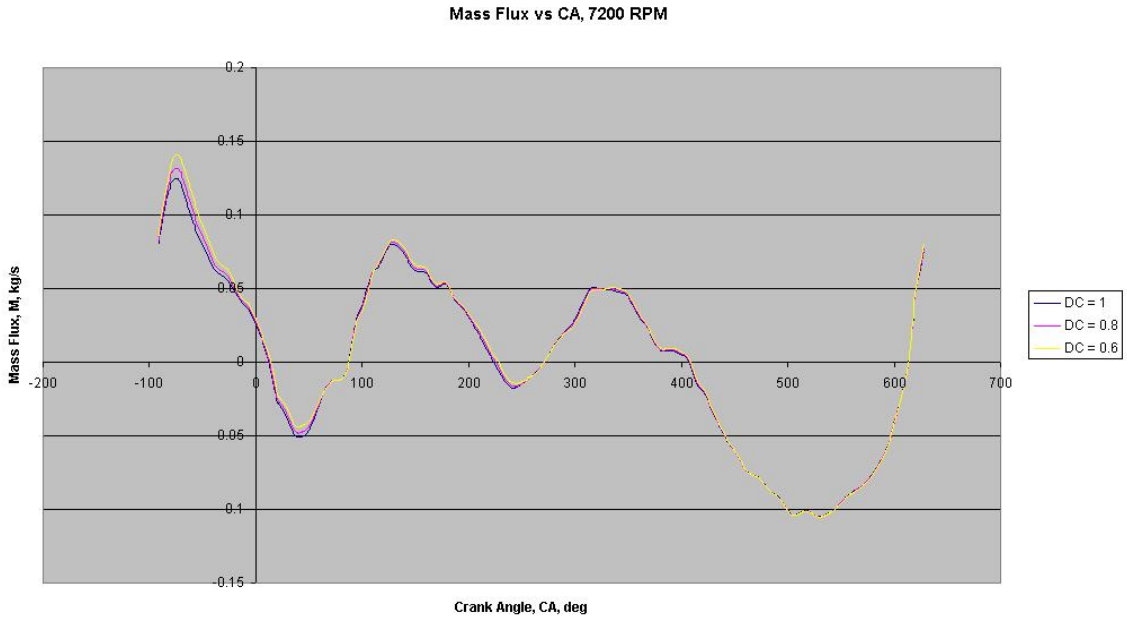
Mass Flux vs CA, 7200 RPM
Mass Flux, M, kg/s
0.2
0.15
0.1
0.05
0
0.05
0.1
0.15
-200
-100
0
100
200
300
400
500
600
700
Crank Angle, CA, deg
DC = 1
DC = 0.8
DC = 0.6

LIST OF REFERENCES

[1] Dvorak, Todd and Hoekstra, Robert (1996). Optimizing Internal Combustion Engine Performance through Response Surface Methodologies. Society of Automotive Engineers *(SAE Paper 962525)* , Warrendale, PA:

[2] Dvorak, Todd and Hoekstra, Robert (2002). Improving Exhaust Header Performance with Multiple Response Surface Methods. PhD Dissertation.

[3] Jemail, Jim (2000). Modeling of a Winston Cup Restrictor Plate Motor Using Ricardo-WAVE Software. Unpublished Master's Thesis: The University of Central Florida.

[4] Brandsteter, Walter R (1969). Similarity Laws for Four-Stroke Engines and Nurnrical Results for the Intake Process Calculated with the Method of Characteristics. Society of Automotive Engineers *(SAE Paper 690466)*, Warrendale, PA:

[5] Tabaczynski, Rodney J (1982). Effects of Inlet and Exhaust System Design on Engine Performance. Society of Automotive Engineers *(SAE Paper 821577)*, Warrendale, PA:

[6] Myers, Raymond H and Montgomery, Douglas C, Response Surface Methodology. John Wiley & Sons, New York, NY (1989).

[7] Selamet, A, Dickey, N. S., Radavich, P. M., and Novak, J. M. (1994) Theoretical, Computational and Experimental Investigation of Helmholtz Resonators: One-Dimensional versus Multi-Dimensional Approach. Society of Automotive Engineers *(SAE Paper 940612)* , Warrendale, PA:

[8] Heisler, Heinz. Advanced Engine Technology. Society of Automotive Engineers, Warrendale, PA *(1995).*

[9] Heywood, John B. Internal Combustion Engine Fundamentals. McGraw-Hill, New York, NY (1988).